

Vibrational line shapes in the amalgamated limit: (para-D₂)_x(ortho-D₂)_{1-x} mixed crystals

J. De Kinder, A. Bouwen, and D. Schoemaker

Physics Department, University of Antwerp (U.I.A.), B-2610 Antwerp (Wilrijk), Belgium

A. Boukahil and D.L. Huber*

Synchrotron Radiation Center, University of Wisconsin-Madison, Stoughton, Wisconsin 53589

(Received 6 December 1993)

The D₂ vibrons have been studied by high-resolution Raman scattering in mixed crystals of (p-D₂)_x(o-D₂)_{1-x}. The o-D₂ and p-D₂ vibrational transitions are found to overlap. Line shapes calculated by the coherent potential approximation are in good qualitative agreement with the experimental data. The linewidth of the o-D₂ transition is much larger than the linewidth of the p-H₂ transition in (o-H₂)_x(p-H₂)_{1-x} mixed crystals with comparable $J = 1$ concentrations. Possible explanations for this difference are discussed.

I. INTRODUCTION

Substitutional disorder can have several effects on the line shape of vibrational transitions. Due to the mismatch in lattice constant, inhomogeneous line broadening of the transition may occur. This can even be seen for isotopic substitution, when motional narrowing occurs.¹ The substitute provides additional vibrational states, which provide new channels for the dephasing of the vibrational transitions, either by population relaxation or by pure dephasing mechanisms. In molecular crystals with a large number of vibrational degrees of freedom, the effects of isotopic substitution are still unresolved.^{2,3} In order to gain more insight into the effect of substitutional disorder, a study of molecular crystals consisting of diatomic molecules was undertaken.^{1,4,5}

In the preceding paper, we reported the results of an investigation of the p-H₂ vibron transition in mixed crystals of (o-H₂)_x(p-H₂)_{1-x} as a function of the o-H₂ concentration.⁵ The width W of the p-H₂ vibron band is $\simeq 4 \text{ cm}^{-1}$, which is smaller than the ortho-para frequency splitting $2\Delta = 6-7 \text{ cm}^{-1}$. This ensures that we are just within the separated band limit.^{6,7} Contrary to solid H₂, the bandwidth of the o-D₂ vibrons ($\Omega_v = 2985 \text{ cm}^{-1}$, Refs. 8 and 9) in solid D₂, $W \simeq 3 \text{ cm}^{-1}$ (Ref. 10) is larger than the energy difference between the p-D₂ and o-D₂ stretching vibrations, $2\Delta = 2.1 \text{ cm}^{-1}$ (Ref. 10). Hence, we extend our work from the separated bands region, viz. our H₂ study,⁵ to the amalgamated region. A stronger coupling between the vibrational states is present, which makes the transition bands overlap. The p-H₂ vibron in (p-D₂)_x(o-D₂)_{1-x} mixed crystals benefits from the same advantages as the p-H₂ in (o-H₂)_x(p-H₂)_{1-x} mixed crystals: (i) far off from other excitations and (ii) absence of inhomogeneous broadening.

In this paper, we will present high-resolution spontaneous Raman scattering measurements of the vibrational states in mixed crystals of (p-D₂)_x(o-D₂)_{1-x} for a varying concentration of p-D₂, from a few percent up to

13.7%. Calculations of the line-shape function in the coherent potential approximation^{5,6} (CPA) were carried out, following an approach identical to that outlined in Ref. 5, with the exception that we have used the full Green's function for an fcc lattice with nearest-neighbor interactions rather than the two-term approximation. The two-term approximation is adequate when the ortho and para peaks are separated, but does not give meaningful results when the peaks overlap, as in the D₂ system.

In the calculation, we wrote the Green's function in the integral form

$$G_o(E) = \int_{-\infty}^{+\infty} dx \frac{\rho(x)}{E-x}, \quad (1.1)$$

which is valid for $\text{Im}(E) \neq 0$. Here $\rho(x)$ denotes the vibron density of states. The connection between Eq. (1.1) and the formal expression for the Green's function given in Ref. 5 [by Eq. (4.3)] is readily established by writing the density of states in terms of the energies of the vibron modes, which we denote by $E(\mathbf{k})$:

$$\rho(x) = \frac{1}{N} \sum_{\mathbf{k}} \delta\{x - [E(\mathbf{k}) - E(0)]\}. \quad (1.2)$$

As in Ref. 5, we neglect differences between the ortho-ortho, ortho-para, and para-para interactions. As a consequence, the density of states depends only on the vibron bandwidth W in pure o-D₂. In evaluating the Green's function from Eq. (1.1), we made use of the analytic approximation for the fcc density of states given by Jelitto¹¹ and calculated the integral numerically using Simpson's Rule with an interval equal to $10^{-4}W$.

The line-shape function depends critically on W and Δ . A fortunate choice of experimental parameters and the closeness of both peaks allowed us to measure the whole vibrational spectrum, whereas for (o-H₂)_x(p-H₂)_{1-x} mixed crystals, only the p-H₂ line shape was measured. As in Ref. 5, we infer Δ from the vibrational fre-

quencies in the dilute gas so that we have $2\Delta = 2.1 \text{ cm}^{-1}$ (Ref. 10). Also, according to Ref. 10, $W = 3 \text{ cm}^{-1}$. A better fit to the data was obtained with a slightly larger value of W , as will be discussed below.

II. EXPERIMENTAL

Research grade D_2 gas (99.4 %) was used as the starting material. The main impurity is $\approx 0.6 \%$ H_2 . Analysis of the starting gas showed that the other impurities were $< 30 \text{ ppm N}_2$, $< 5 \text{ ppm H}_2\text{O}$, and $< 2 \text{ ppm O}_2$. Their concentration in the crystal is expected to be even lower, since they are trapped during the catalysis process.

The concentration of the $o\text{-D}_2$, $p\text{-D}_2$, and the $p\text{-H}_2$ species was determined from the integrated intensity of their respective lowest $\Delta J = 2$ transition in the liquid phase, as measured by spontaneous Raman scattering.^{9,12} The concentration of $p\text{-H}_2$ in the liquid was found to be less than 0.25 %. This difference with the gas phase data is due to the higher boiling point of D_2 .

A description of the experimental setup can be found in Ref. 5. The smaller Stokes shift of the stretching vibration for D_2 allowed us to use the 476-nm line of the Ar^+ laser. No temperature dependence of the signal was found between 5.3 and 12 K. Above 12 K, the measurements were strongly hampered by the sublimation of the crystal.

III. RESULTS

The measured spectra of the vibrational transition in mixed crystals of $(p\text{-D}_2)_x(o\text{-D}_2)_{1-x}$ are shown for a varying concentration of $p\text{-D}_2$ in Fig. 1. Since the interferometry does not provide us with an absolute frequency scale, all the spectra are shifted so that the lowest transition of the $p\text{-D}_2$ molecules occurs at 0 cm^{-1} . The free spectral range (FSR) of the interferometer was set so that it contains both the $p\text{-D}_2$ and the $o\text{-D}_2$ peak, without overlapping orders of interferometry.

The lowest-frequency peak can be related to the $p\text{-D}_2$ transition, while the peak shifted by about 1 cm^{-1} is due to the $o\text{-D}_2$ vibron. The anisotropic interaction in solid D_2 has as leading term the electrostatic quadrupole-quadrupole (EQQ) interaction, which vanishes for all pairs of molecules, except para-para. The resulting shift of the vibrational transition for pairs of $p\text{-D}_2$ molecules is reflected in the splitting of the $p\text{-D}_2$ spectra, which is most prominent for $x = 0.038$. For larger x , contributions from clusters consisting of three and more neighboring $p\text{-D}_2$ molecules also become important. The $o\text{-D}_2$ vibron peak is clearly asymmetric, even at the lowest measured concentration. This asymmetry becomes more pronounced for higher $p\text{-D}_2$ concentrations. The energy difference between the $o\text{-D}_2$ and the $p\text{-D}_2$ peaks increases with increasing x .

The ratio of the intensities of both peaks, which is "anomalously" larger than expected from their respective concentrations, has already been observed in the

literature¹³ and has been analyzed in terms of the ratio of the integrated intensities.^{10,14} The overlap and the asymmetry of the peaks (see Fig. 1) do not allow for a feasible numerical analysis of the data. Therefore, we will not discuss the coupling between the two vibrational modes in terms of intensity ratios. While the original theory^{10,14} was developed only for crystals with isolated impurities, it was recently extended to the mixed crystal regime by the aid of supercell calculations.¹⁵

The theoretical results for the spectra are displayed in Fig. 2 in terms of reduced intensity and relative frequency. All the curves were calculated using the CPA scheme with intramolecular frequency difference, $2\Delta = 2.1 \text{ cm}^{-1}$, and vibron bandwidth, $W = 3.2 \text{ cm}^{-1}$. A comparison with Fig. 1 indicates that the CPA reproduces the dominant two-peak structure at approximately the observed splitting and relative peak heights. That the

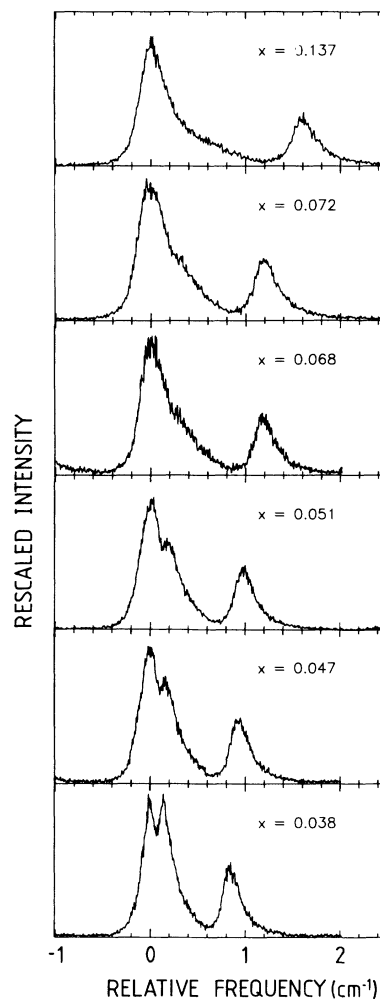


FIG. 1. High-resolution spectra of the vibrational states of the $o\text{-D}_2$ and $p\text{-D}_2$ molecules in mixed crystals of $(p\text{-D}_2)_x(o\text{-D}_2)_{1-x}$ for various x . Since only relative frequency measurements could be performed, all the spectra were shifted so that the lowest $p\text{-D}_2$ transition is at 0 cm^{-1} . The measurements were performed at 7 K. The resolution of the experimental setup is 0.1 cm^{-1} , corresponding to a finesse $\mathcal{F} = 61$.

theory does not account for the splitting of the p - D_2 peak at low para concentrations is to be expected since, as we have noted, the model calculation neglects anisotropic interactions and thus assumes that the para-para interactions are the same as the ortho-ortho and ortho-para interactions.

The value of W that gave the and ortho-para data, 3.2 cm^{-1} , is slightly larger than the value quoted in Ref. 10, 3.0 cm^{-1} . In Fig. 3, we display the curves for $x = 0.038$ for $W = 3.0, 3.1, 3.2, 3.3,$ and 3.4 cm^{-1} . From this figure, it is apparent that when $W = 3.0 \text{ cm}^{-1}$, the ortho peak is noticeably higher than the para peak, in contradiction to the experiment.

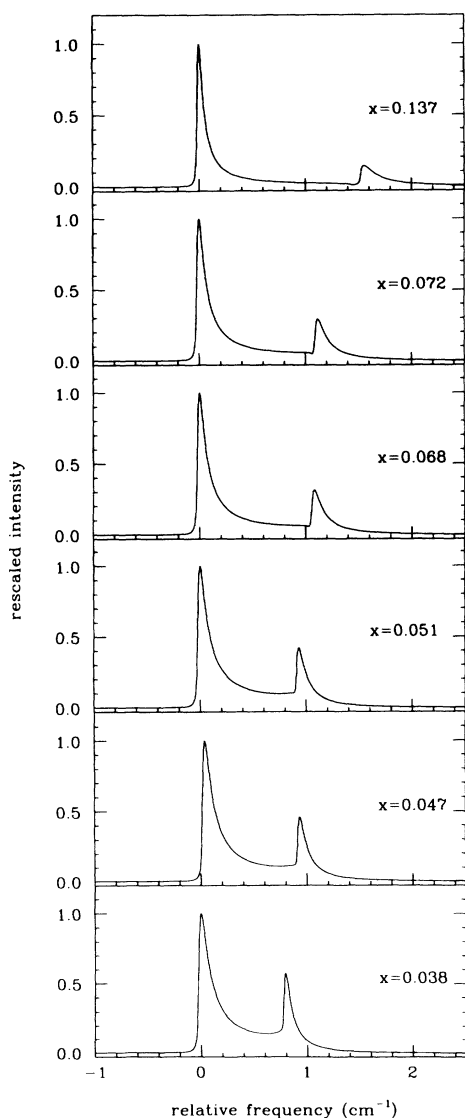


FIG. 2. Theoretical line shapes calculated in the coherent potential approximation for mixed crystals of $(p\text{-D}_2)_x(o\text{-D}_2)_{1-x}$. The curves were obtained with vibron bandwidth $W = 3.2 \text{ cm}^{-1}$ and intramolecular frequency difference $2\Delta = 2.1 \text{ cm}^{-1}$. To ensure convergence in the solutions of the self-consistent equations and simulate the effects of instrumental broadening, the imaginary part of the energy was set equal to 0.1 cm^{-1} (cf. Ref. 5).

IV. DISCUSSION

The results presented in this paper demonstrate the profound effects of compositional disorder on the vibron spectra. These consists of (i) asymmetrical line shapes, (ii) intensities indirectly related to the concentration of

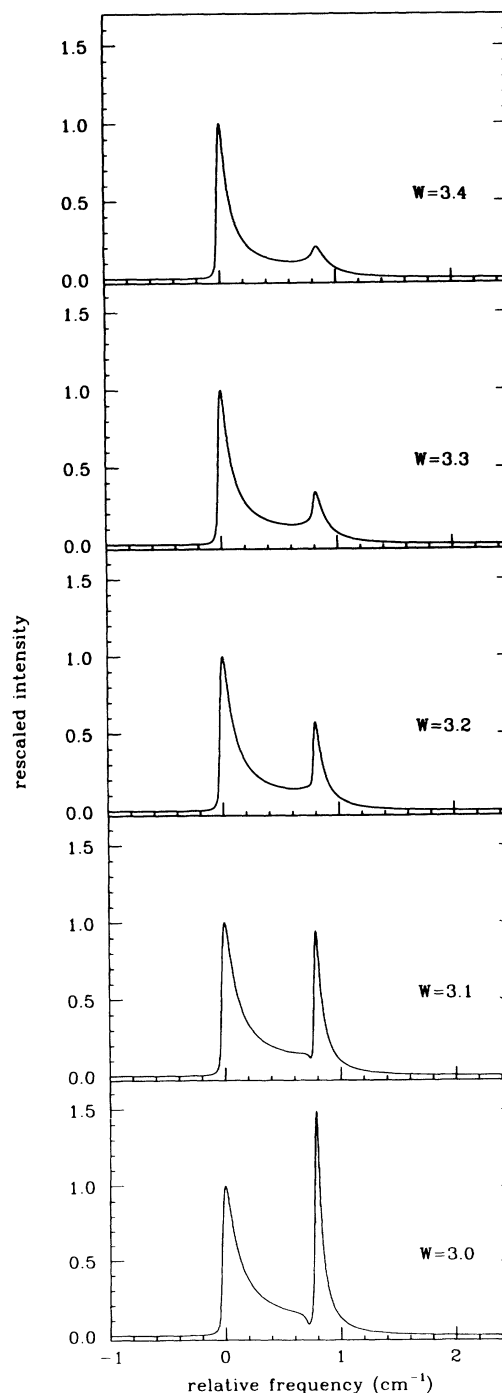


FIG. 3. Theoretical line shapes in the coherent potential approximation for a mixed crystal of $(p\text{-D}_2)_{0.038}(o\text{-D}_2)_{0.962}$ for various values of the exciton bandwidth W . The curves were obtained with intramolecular vibrational frequency difference $2\Delta = 2.1 \text{ cm}^{-1}$ and $\text{Im}E = 0.1 \text{ cm}^{-1}$.

TABLE I. Magnitude of the relative coupling between the two vibrational frequencies in mixed crystals, W/Δ , for various crystals.

Crystal	W/Δ
$(o\text{-D}_2)_x(p\text{-H}_2)_{1-x}$	0.0026 ^a
$(\text{HD})_x(p\text{-H}_2)_{1-x}$	0.015 ^a
$(o\text{-H}_2)_x(p\text{-H}_2)_{1-x}$	1.33 ^a
$(p\text{-D}_2)_x(o\text{-D}_2)_{1-x}$	3.0

^aSee Ref. 5.

the species, and (iii) a change in position of the peaks. Comparing our findings in mixed crystals of H_2 and D_2 , we find that for an equal concentration of dopants, the magnitude of effects (i) and (ii) increases with increasing ratio of the vibron bandwidth to the separation of the intramolecular transition frequencies, i.e., W/Δ . In Table I, we have plotted this value for the various mixed crystals which were investigated.

The spectra calculated by the CPA scheme are in very good qualitative, but not quantitative, agreement with the experimental results. The peak positions are reproduced quite accurately. However, we find that the relative heights of the ortho and para peaks change more rapidly with $p\text{-D}_2$ concentration in the theoretical spectra than in the experimental data. This is probably due to a smearing out of the $p\text{-D}_2$ intensities into a broader peak by the EQQ interactions, which causes a different shift of the vibrational frequency for different clusters of $p\text{-D}_2$ molecules. In addition, the dips in the spectra near the $o\text{-D}_2$ peak for $x \geq 0.068$ appear to be artifacts of the CPA. As noted, Figs. 1 and 2 show the relative positions of the peaks; in Table II, we list the CPA predictions for the absolute positions of the peaks [$E_p(\text{para})$ and $E_p(\text{ortho})$], with the zero of frequency being the vibrational frequency in pure $o\text{-D}_2$.

The $o\text{-D}_2$ linewidths in the $(p\text{-D}_2)_x(o\text{-D}_2)_{1-x}$ mixed crystals are an order of magnitude broader than the linewidths of the $p\text{-H}_2$ vibrons in $(o\text{-H}_2)_x(p\text{-H}_2)_{1-x}$ with comparable $J = 1$ concentration.⁵ A similar difference is seen in the CPA calculations, although the CPA linewidths for D_2 are narrower than the experimental data. The latter difference may be due to the limitations of the CPA, or it may indicate that other line broadening mechanisms are important, a result suggested by the fact that we can get an excellent fit to the experimental

TABLE II. Absolute positions of the peaks [$E_p(\text{para})$ and $E_p(\text{ortho})$] as a function of the $p\text{-D}_2$ concentration with the zero of frequency being the vibrational transition in pure $o\text{-D}_2$.

$x(p\text{-D}_2)$	$E_p(\text{para})$	$E_p(\text{ortho})$
0.038	-0.48	0.31
0.047	-0.53	0.36
0.051	-0.55	0.38
0.068	-0.62	0.46
0.072	-0.64	0.48
0.137	-0.85	0.71

$o\text{-D}_2$ line shape by convoluting the CPA curves with a Lorentzian.

The extra line broadening mechanism cannot involve thermal excitations, since the experimental spectra do not show any temperature dependence. Since the $J = 1$ level, i.e., the ground state of the $p\text{-D}_2$ molecules, is excited, it may play a role in the broadening. The large energy difference between the stretching vibration and the rotations of the $p\text{-D}_2$ molecule makes the decay into other states a high-order process. As a consequence, lifetime broadening is not important, so that the linewidths must result from dephasing processes. These might occur through a vibrational-rotational coupling on the $p\text{-D}_2$ and the strong interaction between the $o\text{-D}_2$ and $p\text{-D}_2$ stretching vibrations.

The general agreement in this paper and in Ref. 5 between the theoretical curves and the experimental data indicates that the CPA provides a reasonably accurate characterization of the Raman spectra. The two features it does not take into account are the splitting of the $J = 1$ ($p\text{-D}_2$ or $o\text{-H}_2$) peak at low impurity concentration and the possible presence of other line broadening processes.

ACKNOWLEDGMENTS

J.D.K. wants to acknowledge financial support from the National Fund for Scientific Research Belgium (NFWO). This work was made possible by further financial support from the Inter-University Institute for Nuclear Sciences (IIKW) and the Belgian national lottery. A.B. and D.L.H. (SRC) received support from the National Science Foundation under the Cooperative Agreement DMR-9212658.

* Also at Department of Physics, University of Wisconsin-Madison, Madison, Wisconsin 53706.

¹ J. De Kinder, E. Goovaerts, A. Bouwen, and D. Schoemaker, Phys. Rev. B **42**, 5953 (1990).

² T.J. Trout, S. Velsko, R. Bozio, P.L. Decola, and R.M. Hochstrasser, J. Chem. Phys. **81**, 4746 (1984).

³ E.L. Chronister and D.D. Dlott, J. Chem. Phys. **79**, 5286 (1983).

⁴ J. De Kinder, A. Bouwen, E. Goovaerts, and D. Schoemaker, J. Chem. Phys. **95**, 2269 (1991); Phys. Rev. B **47**, 14565 (1993).

⁵ J. De Kinder, A. Bouwen, D. Schoemaker, A. Boukahil, and D.L. Huber, preceding paper, Phys. Rev. B **49**, 12754 (1994).

⁶ J. Hoshen and J. Jortner, J. Chem. Phys. **56**, 933 (1972); **56**, 5550 (1972).

⁷ P. Soven, Phys. Rev. **156**, 809 (1967).

⁸ S.S. Bhatnagar, E.J. Allin, and H.L. Welsch, Can. J. Phys. **40**, 9 (1962).

⁹ I.F. Silvera, Rev. Mod. Phys. **52**, 393 (1980).

¹⁰ J. Van Kranendonk, *Solid Hydrogen* (Plenum, New York, 1983), Chap. 3.

- ¹¹ R.J. Jellitto, *J. Phys. Chem. Solids* **30**, 609 (1969).
- ¹² M. Leblans, A. Bouwen, C. Sierens, W. Joosen, E. Goovaerts, and D. Schoemaker, *Phys. Rev. B* **40**, 6674 (1989).
- ¹³ A.H. McKague Rosevear, G. Whiting, and E.J. Allin, *Can. J. Phys.* **47**, 3589 (1967).
- ¹⁴ H.M. James and J. Van Kranendonk, *Phys. Rev.* **164**, 1159 (1967).
- ¹⁵ J.H. Eggert, R.J. Hemley, K.H. Mao, and, J.L. Feldman (unpublished).